Supplemental Experimental Procedures

Contents

General Remarks

Unless otherwise noted, all experiments were conducted under a dry atmosphere of nitrogen to confirm that electrochemistry, rather than oxygen, is the source of oxidative turnover. Reaction cells were assembled in a nitrogen-filled dry box, and all chemicals were used without further purification. Anhydrous acetonitrile was purchased from Millipore Sigma.

^{1}H NMR spectra were obtained at 400 or 600 MHz and chemical shifts were recorded relative to $CHCl_3$ in $CDCl_3$ (δ7.26 ppm). ^{13}C NMR were obtained at 101 MHz. ^{19}F NMR were obtained at 377 MHz. Proof of purity is demonstrated by copies of NMR spectra. NMR multiplicities are reported as follows: singlet (s), doublet (d), triplet (t), quartet (q), multiplet (m), broad signal (br). GC analysis was performed on an Agilent 7890B GC equipped with an HP-5 column (30 m x 0.32 mm x 0.25 µm film) and an FID detector. Quantitative GC analysis was performed by adding dodecane as an internal standard to the reaction mixture upon completion of the reaction. Response factors for the products relative to the internal standard were measured for reaction development.

All electrochemical analyses were carried out in a nitrogen-filled glovebox. Cyclic voltammetry was performed with a Biologic VSP multichannel potentiostat/galvanostat. Cyclic voltammetry was carried out in a three-electrode electrochemical cell, consisting of a glassy carbon disk working electrode (0.07 cm_2 , BASi), a Ag/Ag^+ quasi-reference electrode (BASi) with 0.01 M $AgBF_4$ (Sigma) in MeCN, and a platinum wire counter electrode (23 cm, ALS). The glassy carbon disk electrode was polished in a nitrogen-filled glovebox using diamond polish (15 µm, BASi) and anhydrous MeCN. All experiments were performed at a scan rate of 100 mV/s in a MeCN electrolyte containing 0.1 M KPF_6 unless otherwise noted. Reference electrodes were calibrated against an internal voltage reference of ferrocene (1-10 mM). Reactions were conducted as two-electrode cells with a LANHE LAND battery testing system using nickel foam (1.5 mm x 250 mm x 200 mm, 110 ppi, 99.8% purity, purchased from Amazon.com) and RVC electrodes. Reactions were conducted in Fisherbrand disposable borosilicate glass tubes with a threaded end (16 x 100 mm).

General Procedure for Electrooxidative Fluorination

Conditions A:

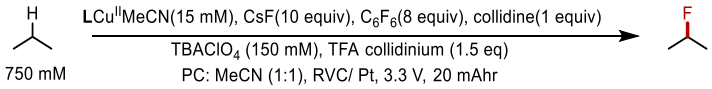

In a nitrogen filled glove box, a 12 mL reaction vial was charged with a stir bar, **L**CuMeCN (26 mg, 45 µmol), CsF (68 mg, 0.450 mmol), hexafluorobenzene (67 mg, 0.360 mmol), collidine (5 mg, 45 µmol), TFA collidinium (16 mg, 66 µmol), $TBAClO_4$ (154 mg, 0.450 mmol), propylene carbonate (1.5 mL) and MeCN (1.5 mL). The solution was allowed to stir for 5 minutes until a blue color was observed. The C-H substrate (3.15 mmol) was then added and briefly stirred. The reaction vial was sealed with a septa-lined cap. Copper wire leads attached to a Pt electrode (6 mm x 30 mm) and an RVC electrode were pierced through the septa. The reaction vial was sealed with a septa-lined cap. The electrodes were submerged to a depth of 5 mm into the solution. An oxidative current was then applied to the Pt electrode (3.3 V, 20 mAh) at 25 °C and vigorously stirred (700 rpm). Following electrolysis, a sample of the solution post electrolysis was analyzed by ^{19}F NMR.

Conditions B:

In a nitrogen filled glove box, a 12 mL reaction vial was charged with a stir bar, LCuMeCN (26 mg, 45 µmol), CsF (102.6 mg, 0.675 mmol), hexafluorobenzene (75 mg, 0.405 mmol), $TBAClO_4$ (154 mg, 0.450

mmol), propylene carbonate (1.5 mL) and MeCN (1.5 mL). The solution was allowed to stir for 5 minutes until a blue color was observed. The C-H substrate (2.25 mmol) was then added and briefly stirred. The reaction vial was sealed with a septa-lined cap. Copper wire leads attached to a Pt electrode (6 mm x 30 mm) and an RVC electrode were pierced through the septa. The reaction vial was sealed with a septa-lined cap. The electrodes were submerged to a depth of 5 mm into the solution. An oxidative current was then applied to the Pt electrode (3.25 V, 20 mAh) at 25 °C and vigorously stirred (700 rpm). Following electrolysis, a sample of the solution post electrolysis was analyzed by ^{19}F NMR.

General Procedure for pyridine TFA salts

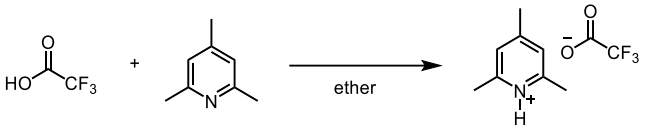

A 20 mL reaction vial was charged with pyridine (18 mmol) and diluted with ether (10 mL). The solution was cooled to 0°C and trifluoroacetic acid (17.9 mmol) was added slowly with a syringe while the solution was stirred vigorously. The reaction was allowed to warm to room temperature and after 10 min a light yellow solid started to precipitate and the vial was placed in the freezer for 2 hours. The solid was then collected by filtration and washed with ether.

Additional Supporting Electrolytes Tested

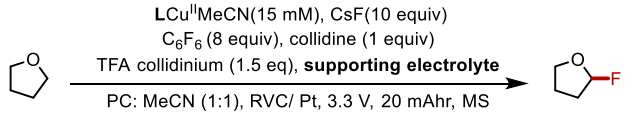

entry	*deviation from standard conditions*	*TON*	*mmol product*
1	50 mM $TBAClO_4$	3.12	0.07 mmol
2	75 mM $TBAClO_4$	4.68	0.11 mmol
3	100 mM $TBAClO_4$	5.64	0.13 mmol
4	200 mM $TBAClO_4$	8.5	0.19 mmol
5	150 mM $TBASO_4H$	-	0
6	150 mM $TBANO_3$	-	0
7	150 mM $TBAIO_4$	<1	0.01 mmol
8	150 mM LiTFSI	-	0
9	75 mM $TBAClO_4$: 75 mM $CsClO_4$	2.3	0.05 mmol
10	150 mM TBAOTf	5.5	0.12 mmol
11	150 mM TBAOAc	<1	0.02 mmol
12	150 mM TMAOAc	2.4	0.05 mmol
13	150 mM TMAF	1.7	0.04 mmol

Figure S1. List of additional supporting electrolytes tested the fluorination conditions. ^{19}F NMR yields are reported using fluorobenzene as an internal standard. 1 TON = 100% yield vs. Cu.

Additional Bases Tested

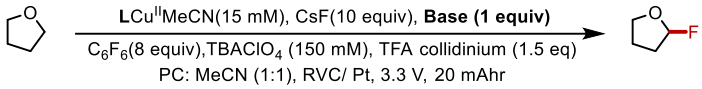

entry	deviation from standard conditions	*TON*	*mmol product*
1	1 equiv. Cs_2CO_3	3.6	0.08 mmol
2	1 equiv. NaO^tBu	2.6	0.06 mmol
3	1 equiv. NaOMe	2.2	0.05 mmol
4	1 equiv. TBA carboxylate	4.9	0.11 mmol
5	1 equiv. DBU	-	0
6	1 equiv. guanidine	<1	0.003 mmol
7	2 equiv. HFIP, 2 equiv. NEt_3	<1	0.003 mmol
8	5 equiv. HFIP, 5 equiv. NEt_3	<1	0.001 mmol
9	1 equiv. methenamine	<1	0.02 mmol
10	1 equiv. tris(2-pyridylmethyl)amine	<1	0.005 mmol
11	1 equiv. 4-amino pyridine	-	0
12	1 equiv. terpyridine	3.6	0.083 mmol
13	1 equiv. 2,6-di-*t*Bu-4-methylpyridine	5.02	0.11 mmol
14	1 equiv. 4-dimethyl amino pyridine	1.6	0.04 mmol
15	1 equiv lutidine	4.06	0.10 mmol

Figure S2. List of additional supporting electrolytes tested under the electrochemical fluorination conditions. ^{19}F NMR yields are reported using fluorobenzene as an internal standard. 1 TON = 100% yield vs. Cu.

Mediators Tested:

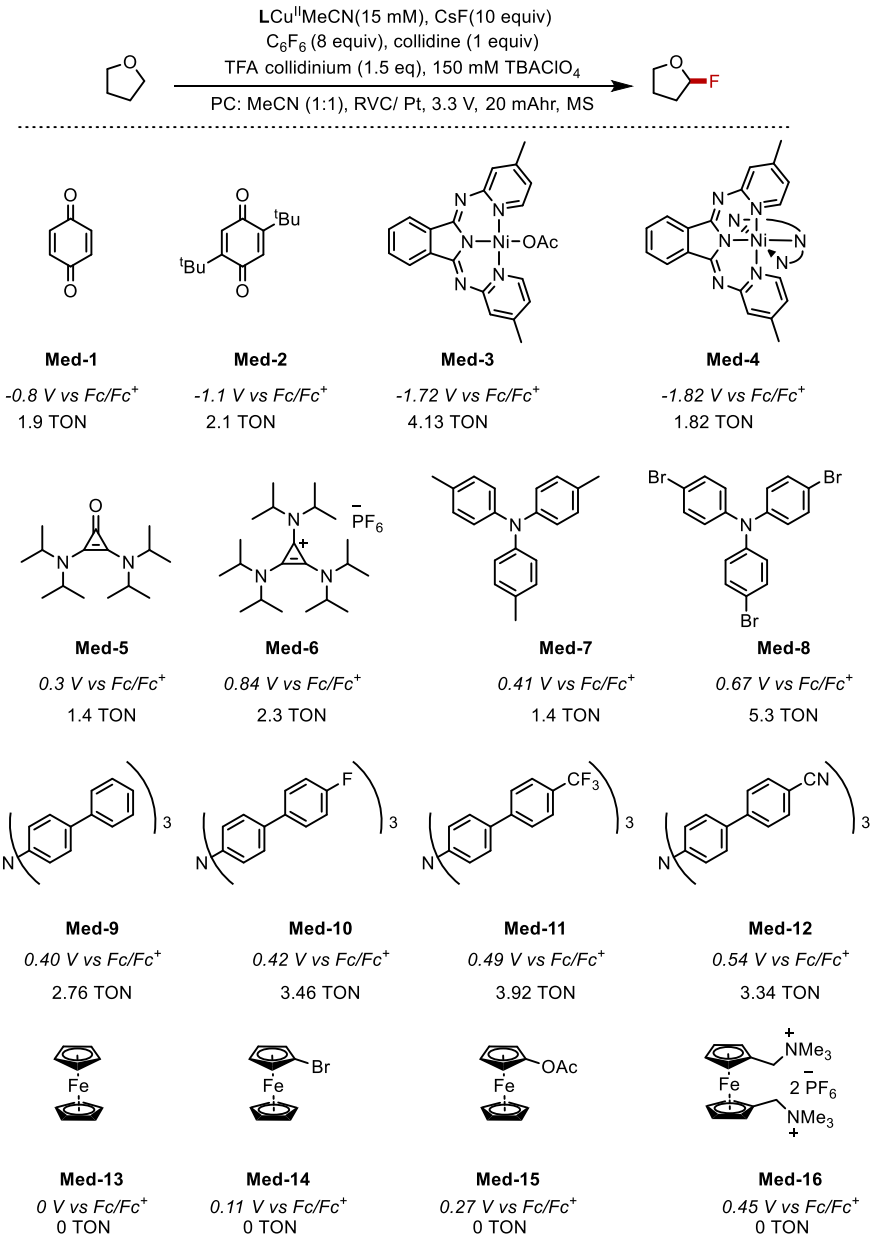

Figure S3. List of additional mediators tested under the the electrochemical fluorination conditions. ^{19}F NMR yields are reported using fluorobenzene as an internal standard. 1 TON = 100% yield vs. Cu.

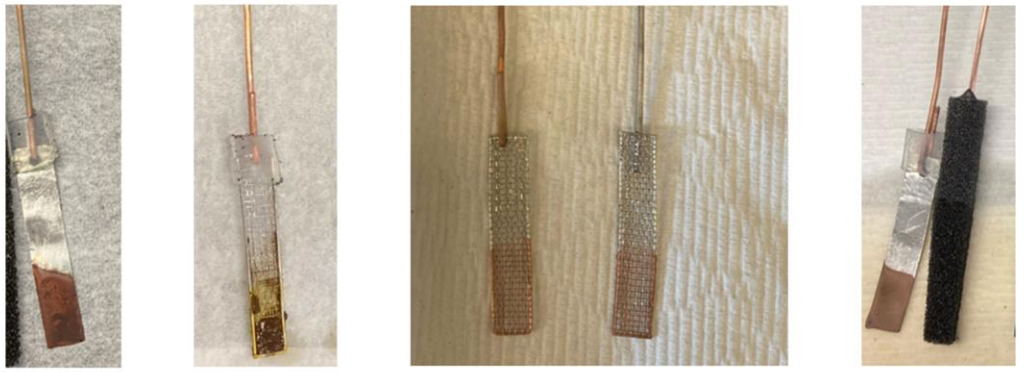

Figure S4. Appearance of the cathode after the reaction under various conditions.

Procedure for Electrode Preparation:

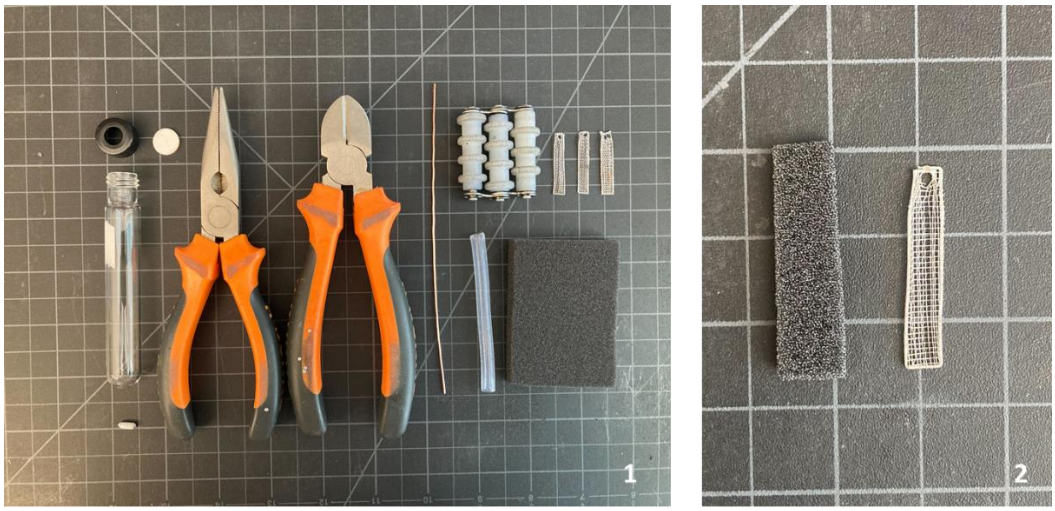

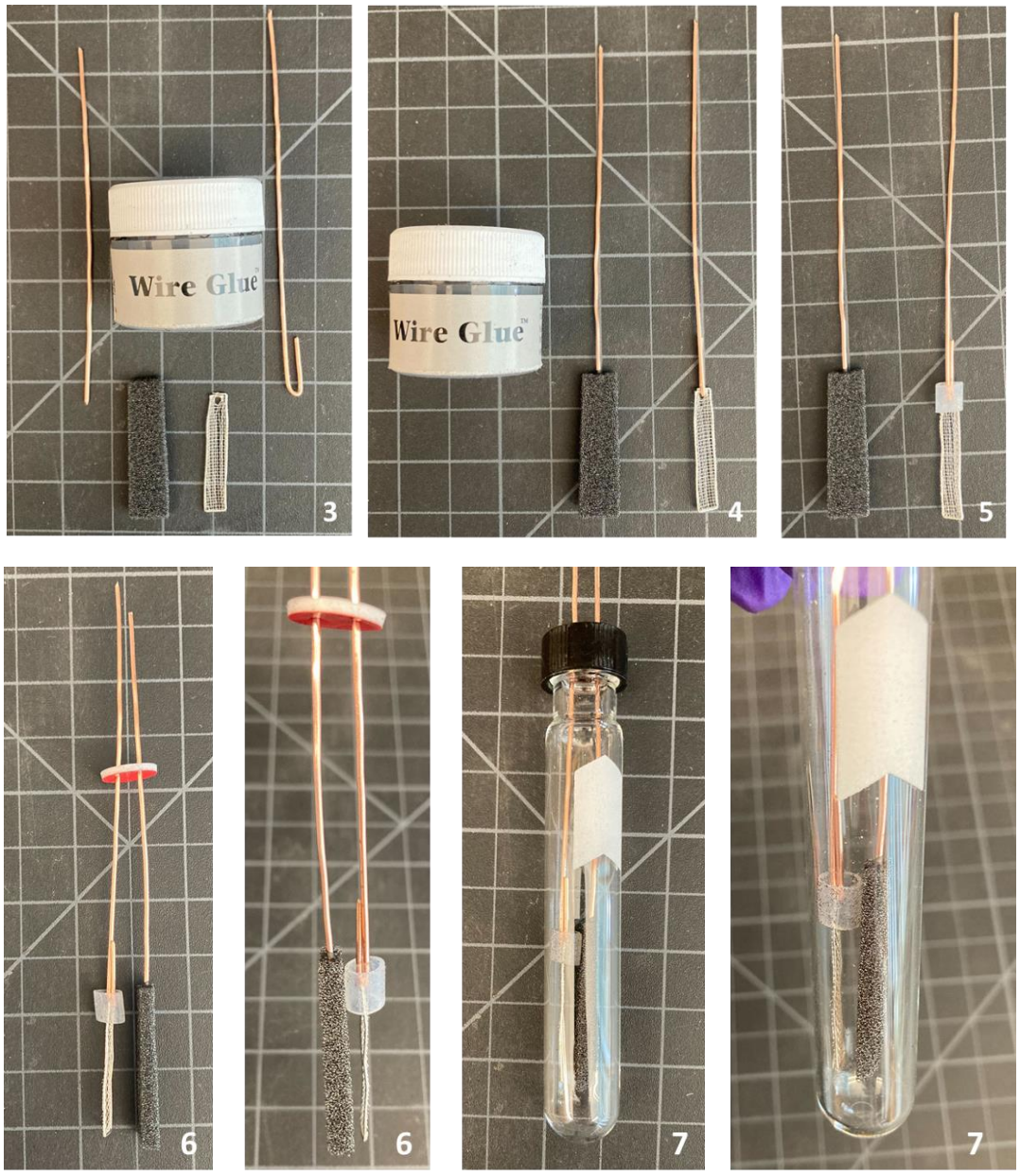

Figure S5. Electrode preparation.

1. Materials required: 12 mL threaded reaction test tube, PTFE septa, threaded test tube cap, copper wire (18 ga), platinum (Pt) mesh, RVC, PTFE tubing (3/16” ID, 1/4” OD, 1/32” WT), pliers, wire glue, wire cutters, 10x3 mm stir bar, wire straighteners, and tin snips.

2. Use a razor to cut the RVC into 6 mm x 32 mm strips. Pt mesh was purchased from Alibaba and came cut into 6 mm x 32 mm strips.

3. Use the wire cutters and wire straightener to cut the Cu wire and straighten the Cu leads.

4. Secure the RVC to the copper wire with wire glue and pierce the Cu wire through the RVC. Thread the Cu wire through the hole of the Pt electrodes and foldback it back on itself to clamp the Pt foam in place.

5. On the platinum anode, a segment of PTFE tubing was cut and was placed over the platinum -copper connection – to prevent the electrodes from touching.

6. Copper wire from the nickel foam and platinum electrodes were pushed through PTFE septa and electrodes were positioned parallel to each other to prevent contact

7. RVC and Pt electrodes were slid into the test tube, inserted until a 1 cm gap remains at the bottom of the test tube. The septa was then secured with the threaded cap.

Incompatible Substrates

Table S1.

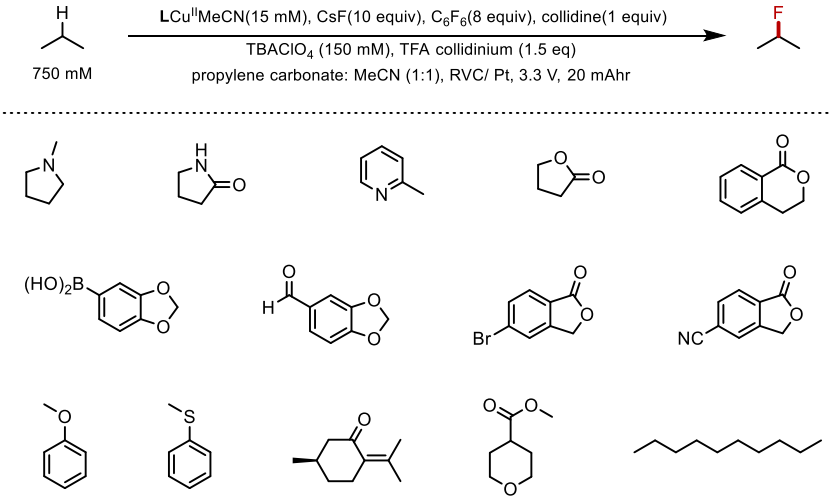

Influence of substrate concentration

Table S2.

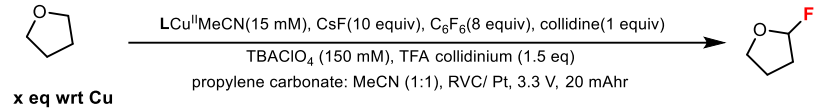

Equiv. THF vs. Cu	[THF] concentration	Yield vs. Cu
15 equiv.	0.225 M	98%
25 equiv.	0.375 M	151%
30 equiv.	0.450 M	277%
50 equiv.	0.750 M	646%
70 equiv.	1.05 M	930%

Performance of other simple Cu salts under optimized condition.

Table S3.

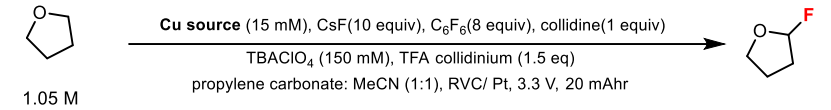

Cu source	Yield vs. Cu
LCu(MeCN)	930%
CuOAc	18%
$Cu(MeCN)_4PF_6$	42%
CuCl	42%
CuI	68%
CuI + bpy	42%
CuI + 1,10-phen	22%
CuI + tpy	46%
$Cu(OAc)_2$	0%
$Cu(OTf)_2$	0%

Characterization of Organic Products

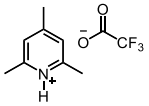

The general procedure to prepare the pyridine TFA salts described above was applied to the reaction of collidine (2.05 g, 16.9 mmol) and trifluoroacetic acid (1.28 mL, 16.8 mmol). The solid was then collected by filtration and washed with ether to yield a white solid (3.10 g, 79%).
^{1}H NMR (400 MHz, $CDCl_3$) δ 7.18 (s, 2H), 2.74 (s, 6H), 2.50 (s, 3H).
^{13}C NMR (101 MHz, $CDCl_3$) δ 162.0 (q, *J* = 35.2 Hz), 157.7, 153.3 (2C), 125.1 (2C), 116.8 (q, *J* = 292.7 Hz), 22.0, 19.3 (2C). 162.02 (q, *J* = 35.2 Hz), 116.79 (q, *J* = 292.7 Hz).
^{19}F NMR (376 MHz, $CDCl_3$) δ -75.77.

1 – 2-fluorotetrahydrofuran

The general procedure for electrochemical C-H fluorination was applied to the reaction of tetrahydrofuran (227 mg, 3.15 mmol). The vial was sealed with the electrodes, removed from the glovebox, and connected to an N_2 line. The reaction was then electrolyzed at 3.3 V for 20 mAh at 25 °C and vigorously stirred (700 rpm). Following electrolysis, a sample of the solution post electrolysis was analyzed by ^{19}F NMR. The yield was determined by ^{19}F NMR yields with fluorobenzene as an internal standard. Characterization data match those of previously reported literature.[1]
^{19}F NMR (400 MHz, $CDCl_3$) δ -111.4 ppm

2 – 2-fluorotetrahydro-2H-pyran

The general procedure for electrochemical C-H fluorination was applied to the reaction tetrahydro-2H-pyran (271 mg, 3.15 mmol). The vial was sealed with the electrodes, removed from the glovebox, and connected to an N_2 line. The reaction was then electrolyzed at 3.3 V for 20 mAh at 25 °C and vigorously stirred (700 rpm). Following electrolysis, a sample of the solution post electrolysis was analyzed by ^{19}F NMR. The yield was determined by ^{19}F NMR yields with fluorobenzene as an internal standard. Characterization data match those of previously reported literature.[1]
^{19}F NMR: (400 MHz, Chloroform-*d*) δ -132.7 ppm

3 – 1-ethoxy-1-fluoroethane

 The general procedure for electrochemical C-H fluorination was applied to the reaction of diethyl-ether (233 mg, 3.15 mmol). The vial was sealed with the electrodes, removed from the glovebox, and connected to an N_2 line. The reaction was then electrolyzed at 3.3 V for 20 mAh at 25 °C and vigorously stirred (700 rpm). Following electrolysis, a sample of the solution post electrolysis was analyzed by ^{19}F NMR. The yield was determined by ^{19}F NMR yields with fluorobenzene as an internal standard.
^{19}F NMR: (376 MHz, Chloroform-*d*) δ -117.94 (dq, *J* = 67.5, 19.7 Hz).

4 – 1-fluoro-1,3-dihydroisobenzofuran

 The general procedure for electrochemical C-H fluorination was applied to the reaction of 1,3-dihydroisobenzofuran (378 mg, 3.15 mmol). The vial was sealed with the electrodes, removed from the glovebox, and connected to an N_2 line. The reaction was then electrolyzed at 3.3 V for 20 mAh at 25 °C and vigorously stirred (700 rpm). Following electrolysis, a sample of the solution post electrolysis was analyzed by ^{19}F NMR. The yield was determined by ^{19}F NMR yields with fluorobenzene as an internal standard.
^{19}F NMR: (376 MHz, Chloroform-*d*) δ -97.73 (dt, *J* = 74.3, 15.4 Hz).

5 – 1-fluoroisochromane

 The general procedure for electrochemical C-H fluorination was applied to the reaction of isochroman (423 mg, 3.15 mmol). The vial was sealed with the electrodes, removed from the glovebox, and connected to an N_2 line. The reaction was then electrolyzed at 3.3 V for 20 mAh at 25 °C and vigorously stirred (700 rpm). Following electrolysis, a sample of the solution post electrolysis was analyzed by ^{19}F NMR. The yield was determined by ^{19}F NMR yields with fluorobenzene as an internal standard.
^{19}F NMR (376 MHz, Chloroform-d) δ -104.87 (d, *J* = 59.1 Hz)

6 – 5-bromo-2-fluorobenzo[1,3]dioxole

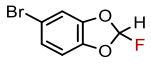 The general procedure for electrochemical C-H fluorination was applied to the reaction of 5-bromobenzo[1,3]dioxole (633 mg, 3.15 mmol). The vial was sealed with the electrodes, removed from the glovebox, and connected to an N_2 line. The reaction was then electrolyzed at 3.3 V for 20 mAh at 25 °C and vigorously stirred (700 rpm). Following electrolysis, a sample of the solution post electrolysis was analyzed by ^{19}F NMR. The yield was determined by ^{19}F NMR yields with fluorobenzene as an internal standard.
^{19}F NMR (376 MHz, Chloroform-d) δ -71.75 (d, J = 44.3 Hz).
GC-MS (m/z): for $C_7H_4BrFO_2$ [M]: calcd 218.0, found 218.1

7 – 3-fluorocyclohexene

 The general procedure (**B**) was modified with acetone as a solvent and 50 equiv of the C-H substrate for electrochemical C-H fluorination was applied to the reaction of cyclohexene (259 mg, 3.15 mmol). The vial was sealed with the electrodes, removed from the glovebox, and connected to an N_2 line. The reaction was then electrolyzed at 3.25 V for 15 mAh at 25 °C and vigorously stirred (700 rpm). Following electrolysis, a sample of the solution post electrolysis was analyzed by ^{19}F NMR. The yield was determined by F NMR yields with fluorobenzene as an internal standard. Characterization data match those of previously reported literature.[2]

^{19}F NMR: (400 MHz, Chloroform-*d*) δ -165.58 ppm

8 – (1-fluorethyl)benzene

The general procedure (**A**) for electrochemical C-H fluorination was applied to the reaction of ethylbenzene (334 mg, 3.15 mmol). The vial was sealed with the electrodes, removed from the glovebox, and connected to an N_2 line. The reaction was then electrolyzed at 3.3 V for 20 mAh at 25 °C and vigorously stirred (700 rpm). Following electrolysis, a sample of the solution post electrolysis was analyzed by ^{19}F NMR. The yield was determined by ^{19}F NMR yields with fluorobenzene as an internal standard (0.02 mmol). Characterization data match those of previously reported literature.[2]
^{19}F NMR: (400 MHz, Chloroform-*d*) δ -166.85 ppm

7 – 9-fluoro-9H-fluorene

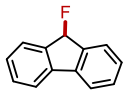

The general procedure (**A**) for electrochemical C-H fluorination was applied to the reaction of fluorene (524 mg, 3.15 mmol). The vial was sealed with the electrodes, removed from the glovebox, and connected to an N_2 line. The reaction was then electrolyzed at 3.3 V for 20 mAh at 25 °C and vigorously stirred (700 rpm). Following electrolysis, a sample of the solution post electrolysis was analyzed by ^{19}F NMR. The yield was determined by ^{19}F NMR yields with fluorobenzene as an internal standard. Characterization data match those of previously reported literature.[2]
^{19}F NMR: (400 MHz, Chloroform-*d*) δ -186.24 ppm (d, *J* = 53.8 Hz)
GC-MS (m/z): for $C_{13}H_8F$ [M-H]: calcd 183.1, found 183.1

10 – 1-(2-fluoropropanyl)-4-methoxybenzene

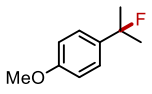

The general procedure (**A**) for electrochemical C-H fluorination was applied to the reaction of 1-isopropyl-4-methoxybenzene (473 mg, 3.15 mmol). The vial was sealed with the electrodes, removed from the glovebox, and connected to an N_2 line. The reaction was then electrolyzed at 3.3 V for 20 mAh at 25 °C and vigorously stirred (700 rpm). Following electrolysis, a sample of the solution post electrolysis was analyzed by ^{19}F NMR. The yield was determined by ^{19}F NMR yields with fluorobenzene as an internal standard.
^{19}F NMR: (400 MHz, Chloroform-*d*) δ -133.76 ppm (hept, *J* = 21.8 Hz)
GC-MS (m/z): for $C_{10}H_{12}FO$ [M-H]: calcd 167.1, found 167.1

11 – 1-fluoro-1,2,3,4-tetrahydronaphthalene

The general procedure (**A**) for electrochemical C-H fluorination was applied to the reaction of 1,2,3,4-tetrahydronaphthalene (423 mg, 3.15 mmol). The vial was sealed with the electrodes, removed from the glovebox, and connected to an N_2 line. The reaction was then electrolyzed at 3.3 V for 20 mAh at 25 °C and vigorously stirred (700 rpm). Following electrolysis, a sample of the solution post electrolysis was analyzed by ^{19}F NMR. The yield was determined by ^{19}F NMR yields with fluorobenzene as an internal standard.
^{19}F NMR: (400 MHz, Chloroform-*d*) δ -155.4 ppm

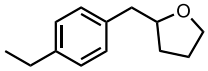

2-(4-ethylbenzyl)tetrahydrofuran

The substrate was prepared according to the literature procedure published by Sevov et. al., *J. Am. Chem. Soc.* **2020**, *142*, 5884. In a nitrogen-filled glove-box, three oven-dried 40 mL vials were each charged with a magnetic stir bar, bis(pyridylamino)isoindolineNiOAc (33 mg, 0.075 mmol, 0.025 equiv), KPF_6 (552 mg, 3.00 mmol, 100 mM), dimethylformamide (30 mL), 1-bromo-4-ethylbenzene (555 mg, 3.00 mmol) and 2-(bromomethyl)tetrahydrofuran (619 mg, 3.75 mmol, 1.25 equiv). The vials were sealed with a septum cap and pierced with a Ni foam cathode and Zn anode. The sealed vial was removed from the glovebox and stirred on a magnetic stir plate at room temperature. A reductive, constant current was applied to the Ni cathode (30 mA, 160.8 mAh, 2.5 equiv e^-). After electrolysis, the solutions were combined in a separatory funnel and extracted with ethyl acetate (3 x 50 mL) and water (75 mL). The organic layers were combined and washed with brine (75 mL). The organic layer was dried over Na_2SO_4, filtered and concentrated by rotary evaporation. The product was purified by flash column chromatography on silica gel (5:95 EA:Hexanes) to afford the product as a colorless oil (1.22 g, 6.41 mmol, 71%).

^{1}H NMR (400 MHz, $CDCl_3$) δ: 7.22 – 7.08 (m, 4H), 4.13 – 4.00 (m, 1H), 3.91 (dddd, *J* = 8.0, 7.0, 6.0, 0.8 Hz, 1H), 3.82 – 3.69 (m, 1H), 2.91 (dd, *J* = 13.6, 6.5 Hz, 1H), 2.73 (dd, *J* = 13.6, 6.5 Hz, 1H), 2.64 (q, *J* = 7.6 Hz, 2H), 2.01 – 1.75 (m, 3H), 1.63 – 1.51 (m, 1H), 1.24 (t, *J* = 7.6, 0.8 Hz, 3H).

^{13}C NMR (101 MHz, $CDCl_3$) δ: 142.0, 136.2, 129.1, 127.8, 80.2, 67.9, 41.6, 31.0, 28.5, 25.6, 15.6.

HRMS-ESI (m/z): for $C_{13}H_{18}O$ [M + H^+]: calcd 191.1430, found 191.1432

2-(4-ethylbenzyl)-5-fluorotetrahydrofuran

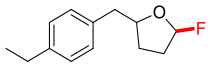

The general procedure (**A**) for electrochemical C-H fluorination was applied to the reaction of 2-(4-ethylbenzyl)tetrahydrofuran (598.5 mg, 3.15 mmol). The vial was sealed with the electrodes, removed from the glovebox, and connected to an N_2 line. The reaction was then electrolyzed at 3.3 V for 20 mAh at 25 °C and vigorously stirred (700 rpm). Following electrolysis, 10.0 μL (0.1066mmol) fluorobenzene was added the solution and mix for 2minutes. A sample of the solution post electrolysis was analyzed by ^{19}F NMR. The yield was determined by F NMR yields with fluorobenzene as an internal standard.

^{19}F NMR: (400 MHz, Chloroform-*d*) δ -110.4 ppm

GC-MS (m/z): for $C_{13}H_{16}FO$ [M-H]: calcd 207.1, found 207.2

2-(4-ethylbenzyl)-2-fluorotetrahydrofuran

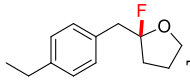

The general procedure (**A**) for electrochemical C-H fluorination was applied to the reaction of 2-(4-ethylbenzyl)tetrahydrofuran (598.5 mg, 3.15 mmol). The vial was sealed with the electrodes, removed from the glovebox, and connected to an N_2 line. The reaction was then electrolyzed at 3.3 V for 20 mAh at 25 °C and vigorously stirred (700 rpm). Following electrolysis, 10.0 μL (0.1066mmol) fluorobenzene was added the solution and mix for 2minutes. A sample of the solution post electrolysis was analyzed by ^{19}F NMR. The yield was determined by F NMR yields with fluorobenzene as an internal standard.

^{19}F NMR: (400 MHz, Chloroform-*d*) δ -106.1 ppm

GC-MS (m/z): for $C_{13}H_{16}FO$ [M-H]: calcd 207.1, found 207.2

Kinetic studies of HAT by LCu^{III}F

UV-vis spectra were collected on an Agilent Cary 60 spectrophotometer outfitted with a Unisoku Unispeks cryostat (−100 °C to + 100 °C). **L**Cu^{III}F was generated in situ by the reported procedure.[3] A

dichloromethane solution of [TBA]**L**Cu^{II}F (0.1 mL, 3.0 mM) was diluted to 2.700 mL in a quartz cuvette under a nitrogen atmosphere. The cuvette was sealed with a septum cuvette and cooled to −30 °C in the UV-Vis spectrometer. A dichloromethane solution of the oxidant [NAr$_3$]PF$_6$ (Ar = 4-bromophenyl) (0.1 mL, 3.0 mM) was injected into the cuvette, and the corresponding optical features of **L**Cu^{III}F were observed, Then, a solution of the C-H substrate (0.2 mL, 225 mM, 100 equivalents) was then injected into the cuvette by syringe. The decay of the absorption maximum of **L**Cu^{III}F at 820 nm was monitored.

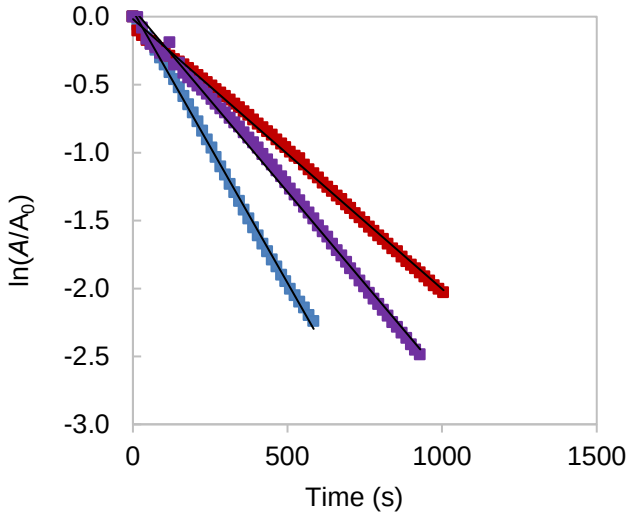

Figure S6. Kinetic traces for the reaction of **L**Cu^{III}F with xanthene (blue 100 eq R^2 = 0.999; purple 75 eq R^2 = 0.996; red 50 eq R^2 = 0.998).

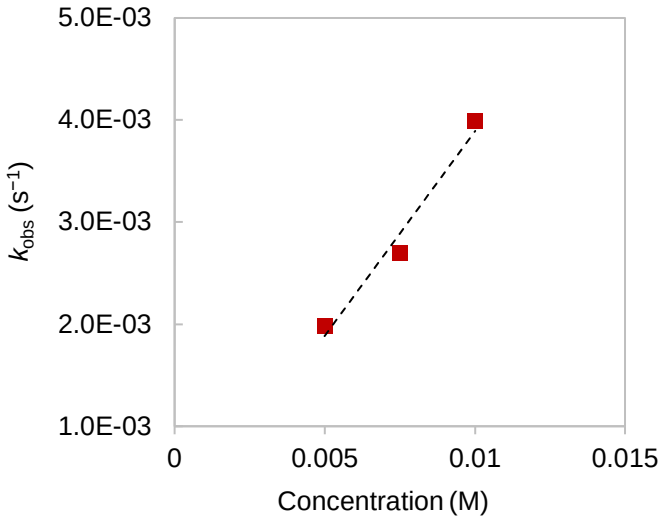

Figure S7. Plot of k_{obs} vs concentration of xanthene for the reaction of **L**Cu^{III}F with xanthene (R^2 = 0.972).

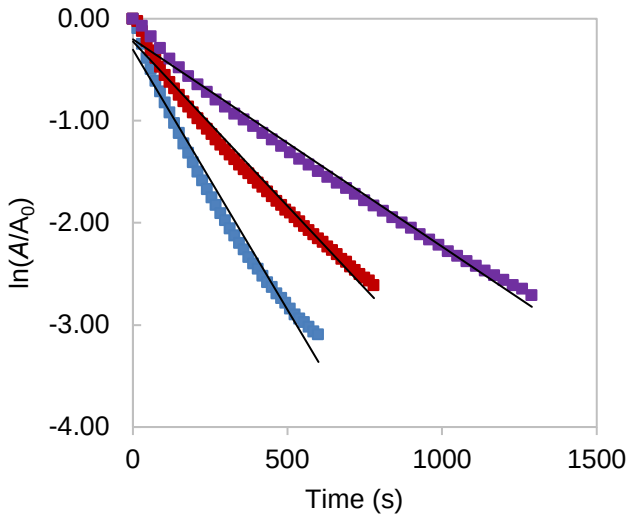

Figure S8. Kinetic traces for the reaction of **L**Cu^{III}F with 9,10-dihydroanthracene (purple 100 eq R^2 = 0.991; red 200 eq R^2 = 0.986; blue 300 eq R^2 = 0.978).

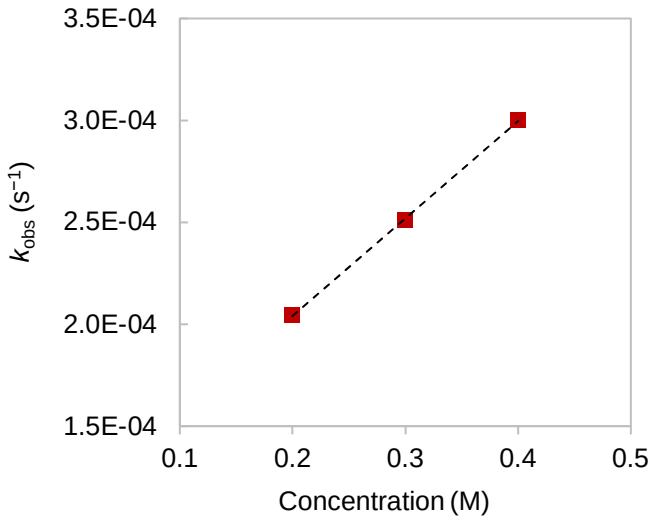

Figure S9. Plot of k_{obs} vs concentration of 9,10-dihydroanthracene for the reaction of **L**Cu^{III}F with 9,10-dihydroanthracene (R^2 = 0.982).

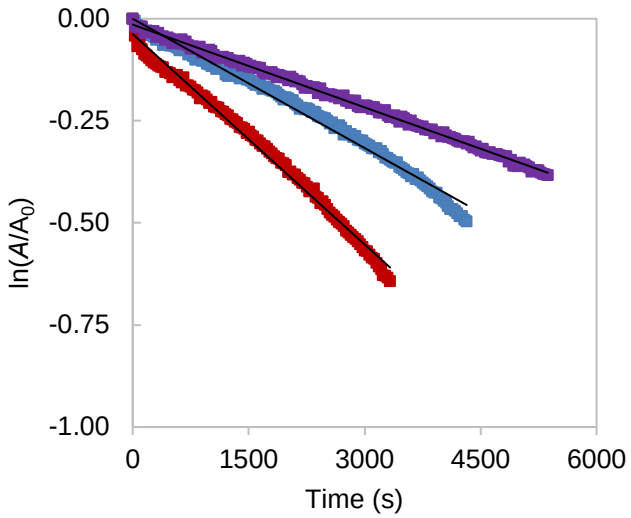

Figure S10. Kinetic traces for the reaction of **L**Cu^{III}F with fluorene (purple 100 eq R^2 = 0.998; blue 200 eq R^2 = 0.988; red 50 eq R^2 = 0.992).

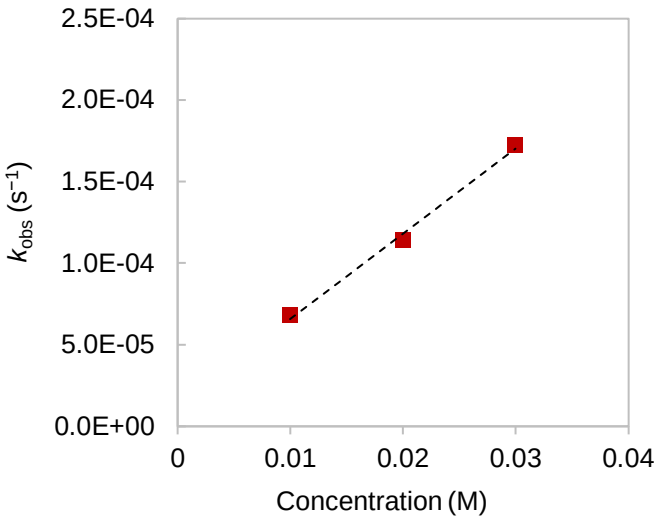

Figure S11. Plot of k_{obs} vs concentration of fluorene for the reaction of **L**Cu^{III}F with fluorene (R^2 = 0.995).

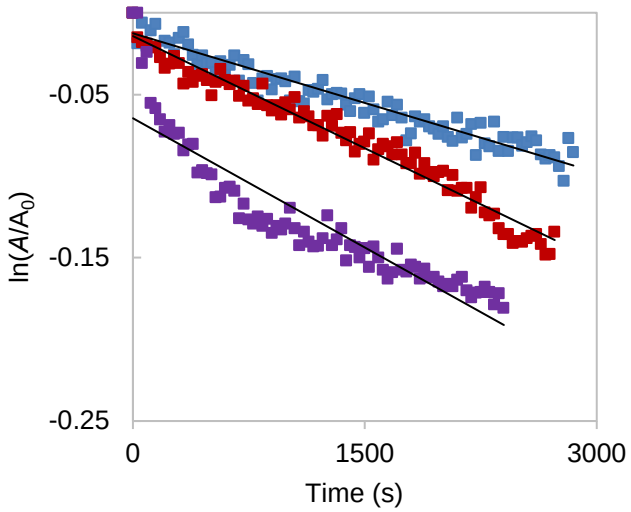

Figure S12. Kinetic traces for the reaction of **L**Cu^{III}F with toluene (blue 3000 eq R^2 = 0.882; red 4000 eq R^2 = 0.967; purple 5000 eq R^2 = 0.831).

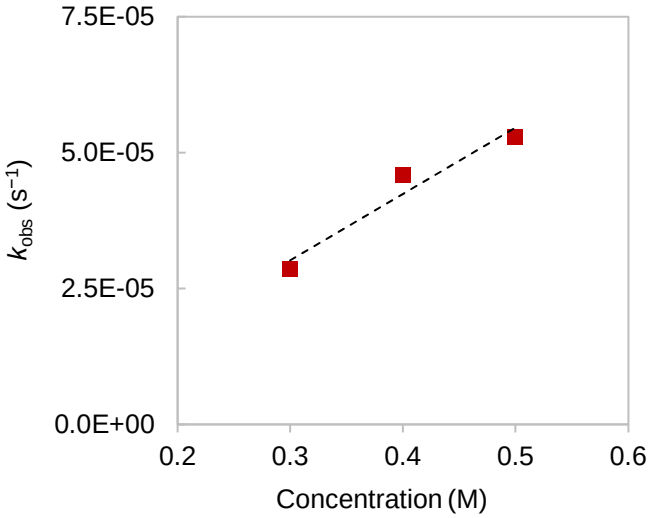

Figure S13. Plot of k_{obs} vs concentration of toluene for the reaction of **L**Cu^{III}F with toluene (R^2 = 0.943).

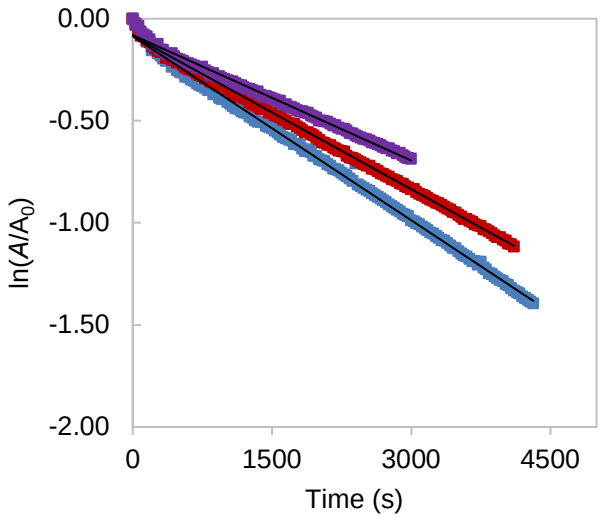

Figure S14. Kinetic traces for the reaction of **L**Cu^{III}F with THF (purple 2000 eq R^2 = 0.993; red 3000 eq R^2 = 0.999; blue 4000 eq R^2 = 0.998).

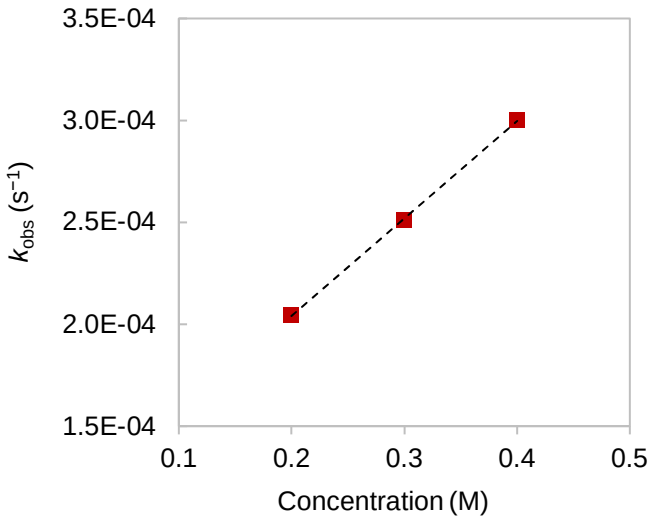

Figure S15. Plot of k_{obs} vs concentration of THF for the reaction of **L**Cu^{III}F with THF (R^2 = 0.999).

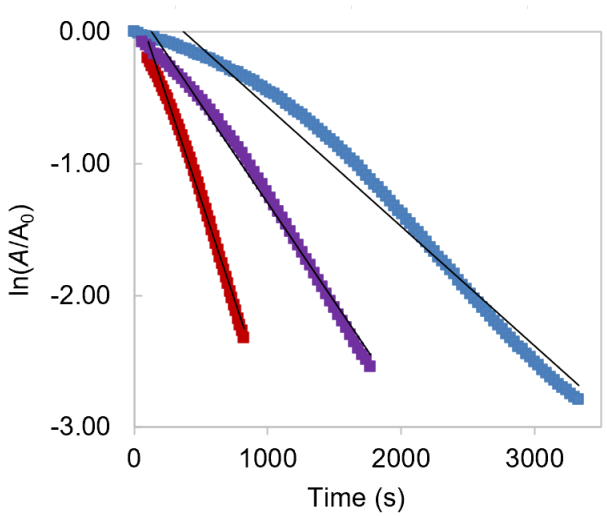

Figure S16. Kinetic traces for the reaction of **L**Cu^{III}F with pthalan (red 0.045 M substrate R^2 = 0.9934; purple 0.03 M substrate R^2 = 0.9904; blue 0.015 M substrate R^2 = 0.9767).

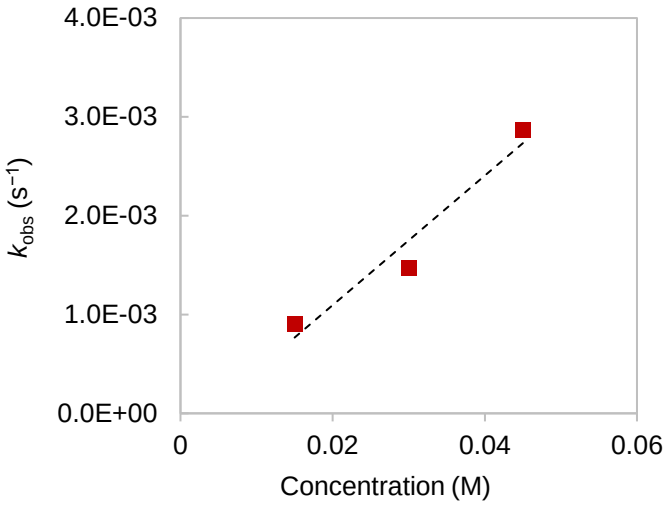

Figure S17. Plot of k_{obs} vs concentration of THF for the reaction of **L**Cu^{III}F with pthalan (R^2 = 0.9437). y = 0.0656x - 0.0002

Table S4. Second order rate constants, k_2, for the reaction of **L**Cu^{III}F and C-H substrates

Substrate	k_2 (M^{-1} s^{-1})
xanthene	0.40 (7)
9,10-dihydroanthracene	0.077 (10)
fluorene	0.0052 (3)

toluene	0.00012 (3)
THF	0.00048 (1)
pthalan	0.066(16)

Measurement of the half-lives of LCu^{III}-F in various solvents

LCu^{III}F was generated in situ by the reported procedure in dichloromethane.[3] A cooled dichloromethane solution of [NAr$_3$]PF$_6$ (Ar = 4-bromophenyl) (21.9 mg, 0.0349 mmol) was added to a cooled solution of [TBA]LCuF (28.2 mg, 0.0349 mmol) at -40 °C and stirred for 30 seconds. The mixture was placed in a -40 °C freezer for 20 minutes. All volatiles were removed in vacuo to give a dark solid, which was extracted into various solvents, including DCM, acetone, MeCN, and PC. The half-life of **L**Cu^{III}F was determined by measuring a UV-vis spectrum every 1 min at 22 °C. The ln[A] vs. t plots yield the first-order rate constants of **L**Cu^{III}F self-decay in various solvents, which can be used to calculate the half-lives using $t_{1/2} = 0.693/k_{decay}$. The decay of **L**Cu^{III}F in acetone is too fast to measure at 22 °C, as the **L**Cu^{III}F has fully decomposed at the time the first UV-vis spectrum was measured. Therefore, we estimate the $t_{1/2}$ of **L**Cu^{III}F is less than 30 s.

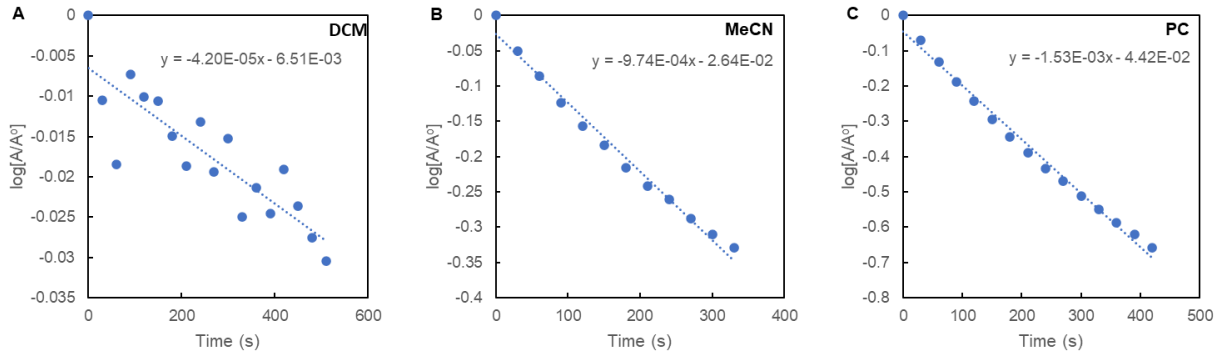

Figure S18. Plots of log[A/A°] vs. *t* for the self-decay **L**Cu^{III}F complex in (A) DCM, (B) MeCN, and (C) PC.

General Procedure for evaluating the formation of the [LCu^{II}F]$^-$ from F sources.

A 20 ml reaction vial was charged with **L**CuMeCN (8.8 mg, 0.015 mmol, 1.0 eq), CsF or KF (0.15 mmol, 10 eq). The corresponding solvents (5 mL) was added to the vial and the solution was stirred for 3 mins. The resulting suspension was filtered and transferred to a cuvette for UV-vis measurement under room temperature. The yield was calculated by simulation of the UV-vis spectra with the UV-vis profiles of **L**CuMeCN and TBA[**L**Cu^{II}F] in the corresponding solvents.

Table S5. Evaluation the [**L**Cu^{II}F]$^-$ formation.

Entry	Solvent	F$^-$ Source	Recovery of **L**CuMeCN	Yield of [**L**Cu^{II}F]$^-$
1	DCM	CsF	56%	40%
2	Acetone	CsF	4%	67%
3	PC	KF	57%	32%
4	PC	CsF	0%	74%
5	MeCN	CsF	11%	78%

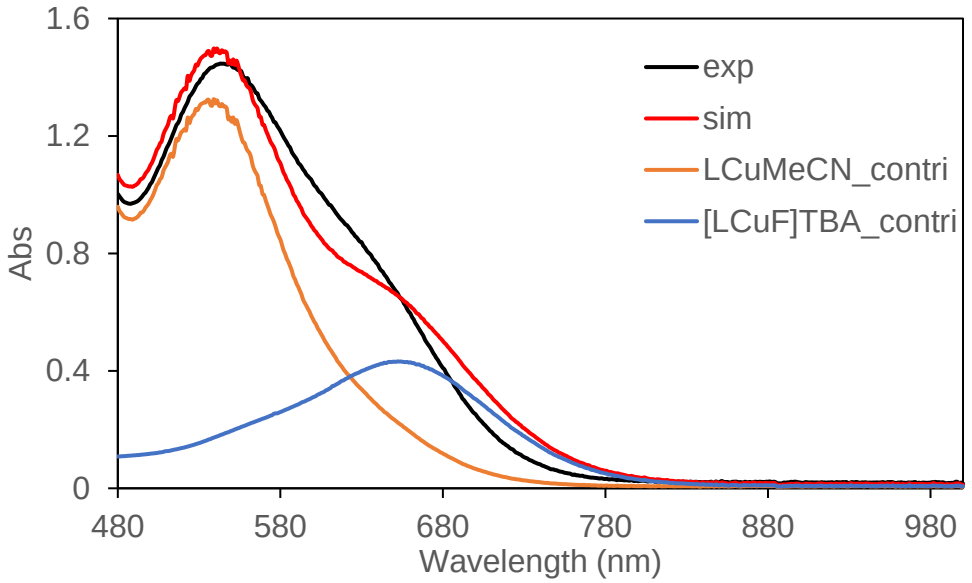

Figure S19. UV-vis spectra of $[LCu^{II}F]^-$ formation with CsF in DCM (entry 1).

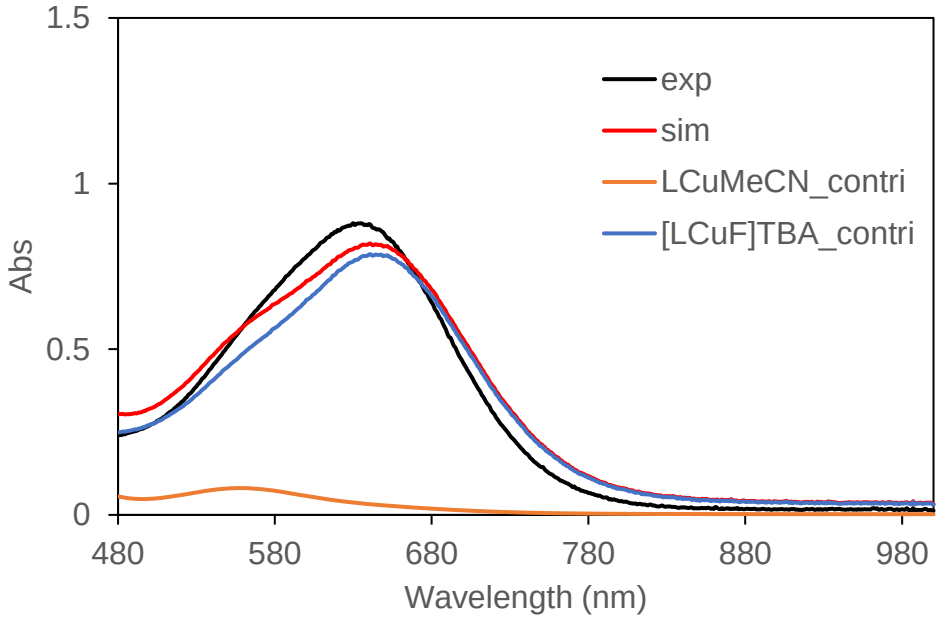

Figure S20. UV-vis spectra of $[LCu^{II}F]^-$ formation with CsF in acetone (entry 2).

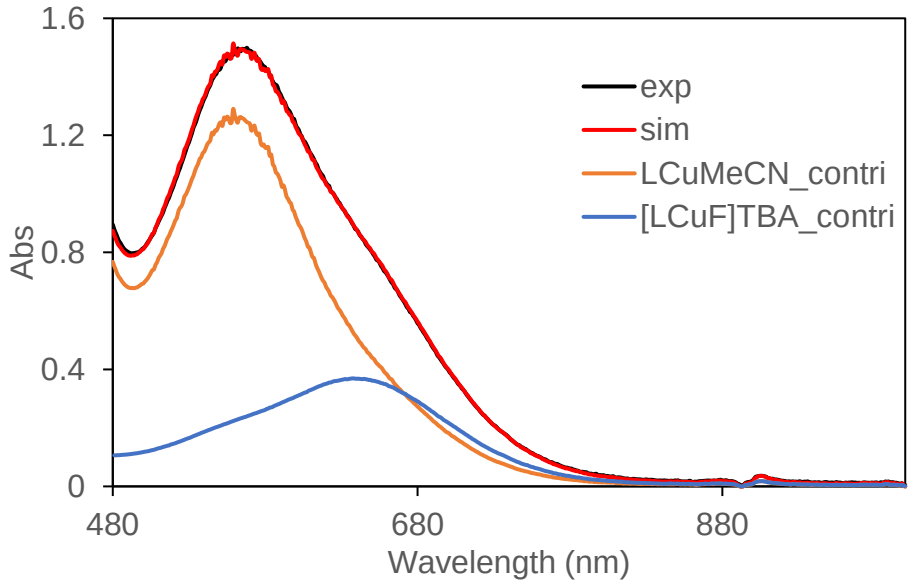

Figure S21. UV-vis spectra of $[LCu^{II}F]^-$ formation with KF in PC (entry 3).

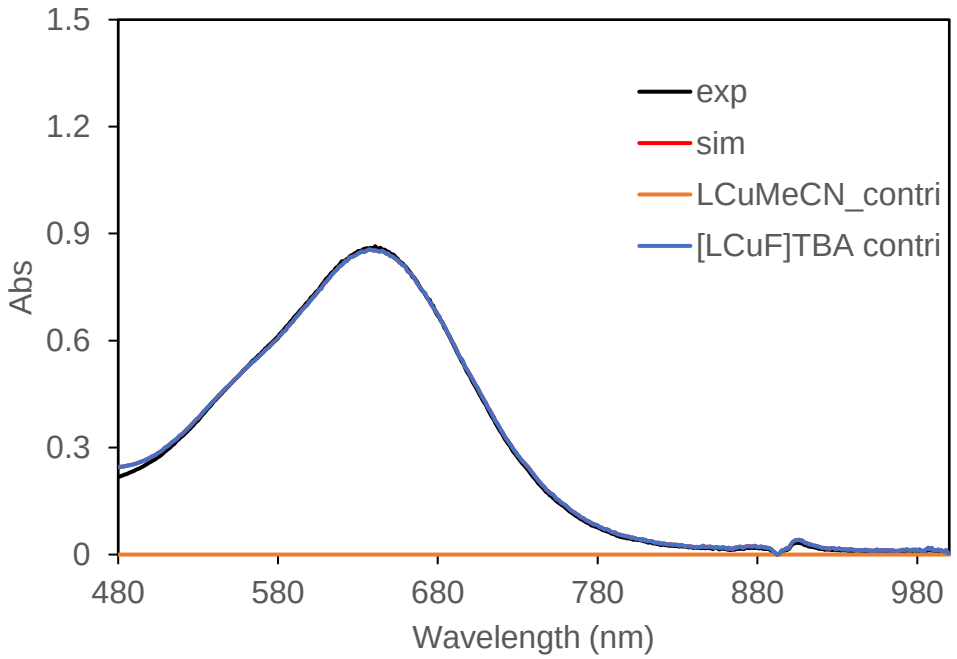

Figure S22. UV-vis spectra of $[LCu^{II}F]^-$ formation with CsF in PC (entry 4)

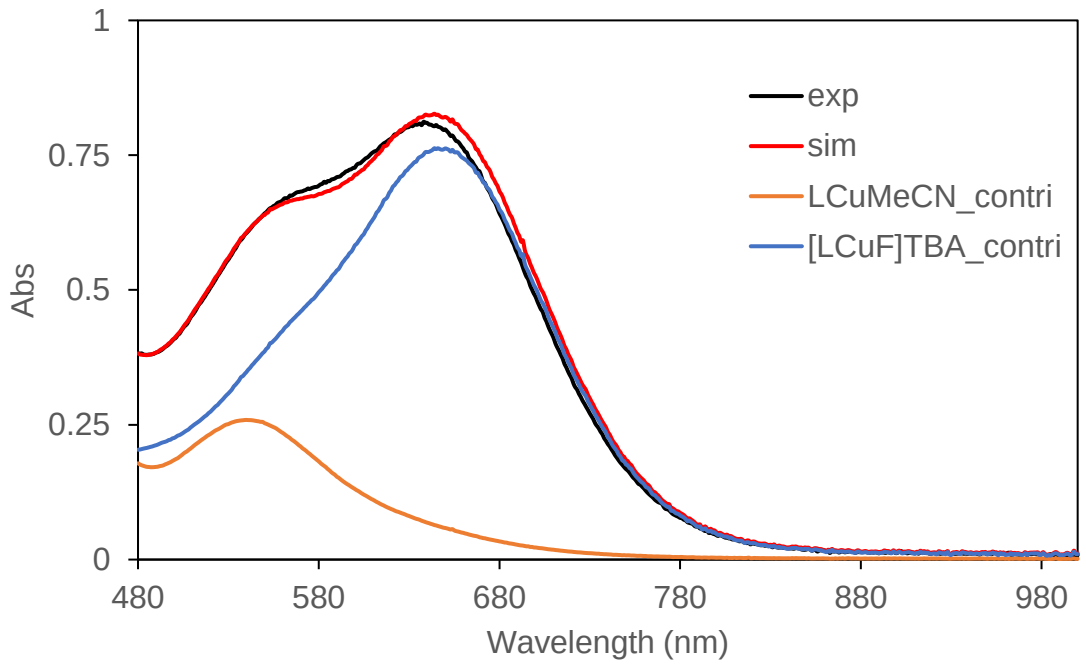

Figure S23. UV-vis spectra of $[LCu^{II}F]^-$ formation with CsF in MeCN (entry 5)

Computational Details

All DFT calculations were performed in ORCA.[4] Geometry optimizations were performed at the B3LYP/6-31G(d) (SDD for Cu) level of theory with D3BJ dispersion correction. A frequency calculation was then performed on the optimized structures at the same level of theory, confirming the absence of imaginary frequencies. A single point energy calculation on the optimized structure was then performed at B3LYP/def2-TZVP (SDD for Cu) level of theory, with CPCM solvent modeling (dichloromethane) and D3BJ dispersion correction. Calculation of asynchronicity factor was performed as previously reported for related formally copper(III) complexes.[5,6] The computed bond dissociation free energies were benchmarked to the experimental value of DHA (76.3 kcal/mol).

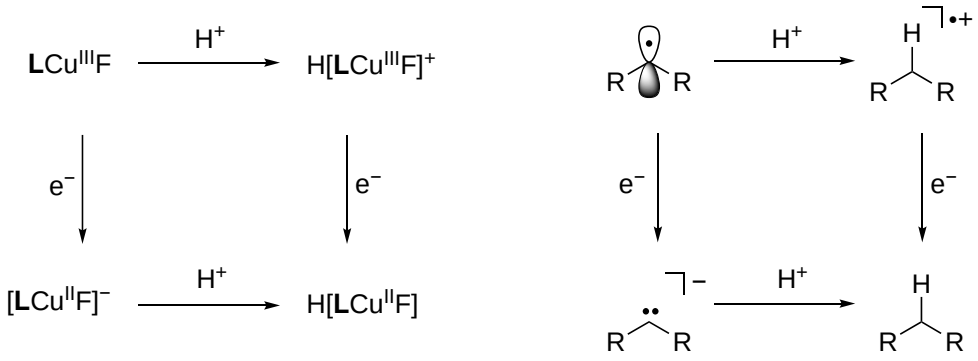

Asynchronicity Factor (η) $= 1/\sqrt{2}\,[-G(Cu^{II}F^-) + G(Sub^-) + G(Cu^{III}FH^+) - G(SubH^+)$

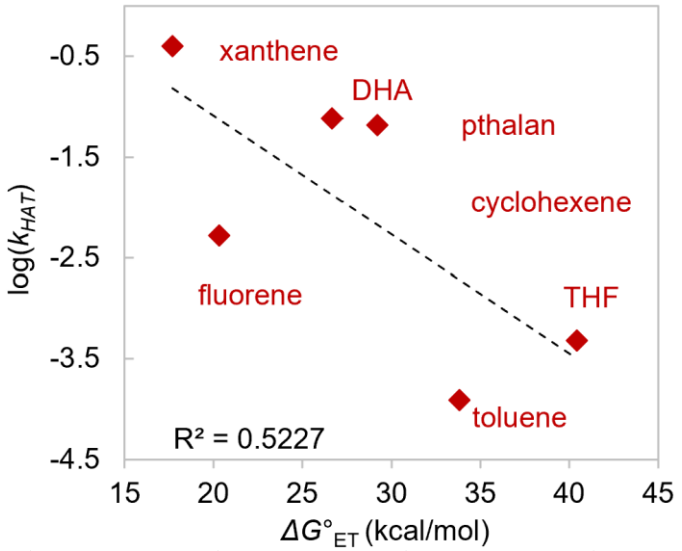

Figure S24. Plot of log(k_2) vs. computed ΔG^o_{ET} of C-H substrates.

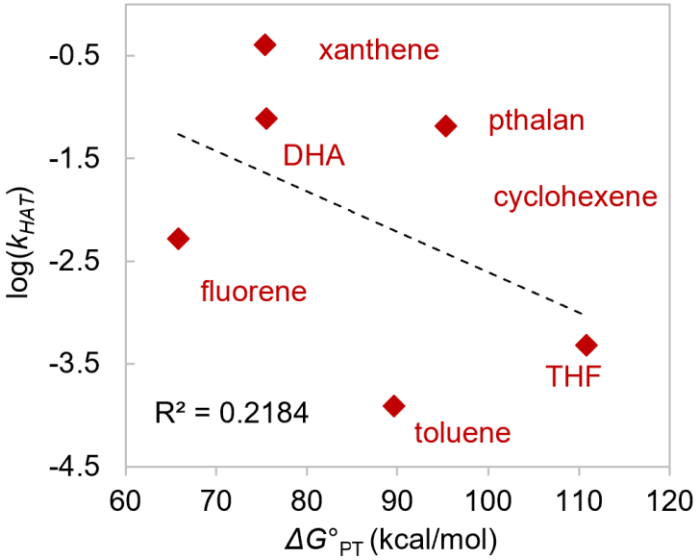

Figure S25. Plot of log(k_2) vs. computed ΔG^o_{PT} of C-H substrates.

Anderson's model (*Chem. Sci.* **2021**, *12*, 4173-4183)

$$\Delta G^{\ddagger} = x\,\Delta G_{PCET} + y\,\Delta G_{ET} + z\,\Delta G_{PT}$$

According to Anderson's model, the best fit that we observe is when x = 1, y = 0, z = 0. This is presumably because the fit for log(k_{obs}) vs ΔG_{PCET} is much better than the fits with ΔG_{PT} (R^2 = 0.2184) or ΔG_{ET} (R^2 = 0.5227). Thus, this plot reflects the log(k_{obs}) vs ΔG_{PCET} as shown above.

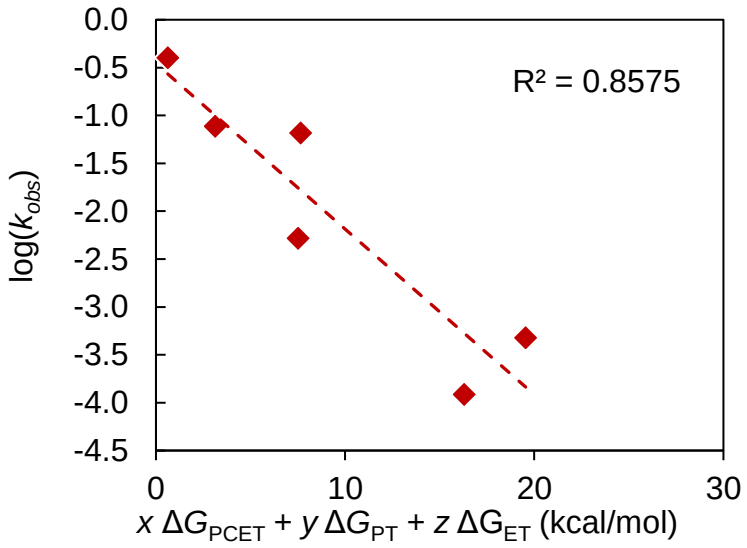

Figure S26. Plot of the best fit for experimental log(k_{obs}) vs calculated $x\ \Delta G_{PCET} + y\ \Delta G_{ET} + z\ \Delta G_{PT}$ (x = 1, y = 0, z = 0) for **L**Cu^{III}F and C-H substrates. R^2 = 0.8575

Borovik's model (*PNAS* **2021**, *118*, e2108648118)

$$\Delta G^{\ddagger} = \alpha(\Delta G_{ET} + x\,\Delta G_{PT}) + \beta$$

According to Borovik's model, the best fit that we observe is when x = 0. This is presumably because the poor fit for log(k_{obs}) vs ΔG_{PT} (R^2 = 0.2184). Thus, this plot reflects the log(k_{obs}) vs. ΔG_{ET} as shown above.

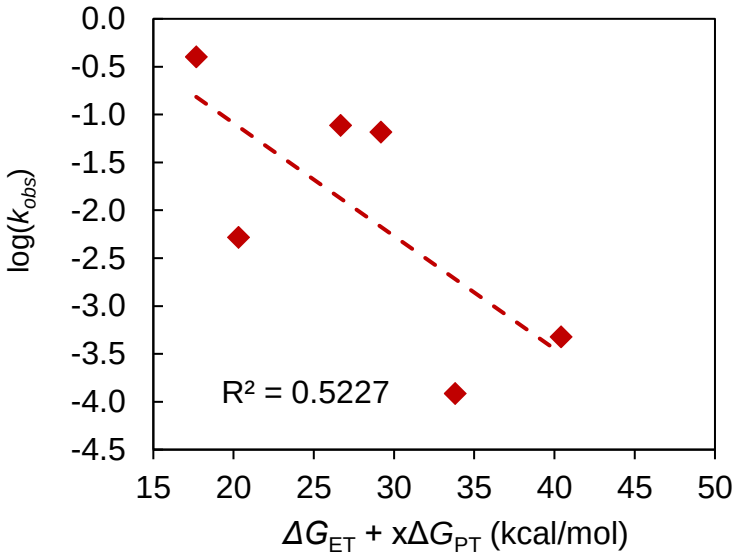

Figure S27. Plot of the best fit for experimental log(k_{obs}) vs calculated $\Delta G_{ET} + x\,\Delta G_{PT}$ (x = 0) for **L**Cu^{III}F and C-H substrates. R^2 = 0.5227.

Table S6. Gibbs energies of species for the calculation of asynchronicity factor.

Compound	*G* (hartree)
LCu^{III}FH+	−1813.536
LCu^{II}F−	−1813.323
LCu^{III}F	−1813.348
LCu^{II}FH	−1813.958
xanthene	-576.404
xanthene•	-575.794

xanthene-	-575.892
xanthene+	-576.195
fluorene	-501.191
fluorene•	-500.57
fluorene-	-500.694
fluorene+•	-500.978
toluene	-271.422
toluene•	-270.786
toluene-	-270.887
toluene+•	-271.187
THF	-232.33
THF•	-231.69
THF-	-231.762
THF+•	-232.086
pthalane	-384.72
pthalane•	-384.098
pthalane-	-384.176
pthalane+•	-384.492
Chromane	-424.01
Chromane• (ether C-H bond)	-423.367
Chromane- (ether C-H bond)	-423.448
Chromane+•	-423.799
Chromane	-424.01

Chromane• (benzylic C-H bond)	-423.382
Chromane- (benzylic C-H bond)	-423.472
Chromane+•	-423.799

Tetraline	-388.072
Tetraline•	-387.443
Tetraline-	-387.537
Tetraline+•	-387.844

Table S7. Calculated electron transfer driving force asynchronicity factor for the reaction of **L**$Cu^{III}F$ and C-H substrates

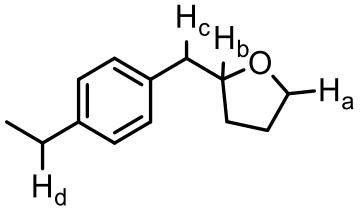

Substrate	ΔG_{ET} (eV)	ΔG_{PT} (eV)	ΔG_{PCET} (kcal/mol)	η (V)
9,10-dihydroanthracene	0.98	2.77	3.12	1.491
toluene	1.24	3.29	16.3	1.390
xanthene	0.65	2.77	0.622	1.762
fluorene	0.74	2.42	7.50	1.390
THF	1.49	4.07	19.5	2.151
pthalane	1.07	3.50	7.65	2.021
12 C-H_a	1.00	4.35	23.0	2.78
13 C-H_b	1.00	4.21	17.8	2.67
14 C-H_c	1.00	3.31	13.8	1.91
15 C-H_d	1.00	3.40	12.2	1.99
tetraline	1.07	3.29	11.8	1.842

Table S8. Benchmarking calculated asynchronicity factors with the reported copper(III) carboxylate complex, **L**$Cu^{III}O_2CAr$.[5]

Substrate	η (V) (This work)	η (V) (from ref[5])
9,10-dihydroanthracene	1.126	0.993
toluene	1.339	----
xanthene	1.392	----
fluorene	1.035	----
THF	1.785	----

References

1. Beniazza, R., Abadie, B., Remisse, L., Jardel, D., Lastécouères, D., and Vincent, J.-M. (2017). Light-promoted metal-free cross dehydrogenative couplings on ethers mediated by NFSI: reactivity and mechanistic studies. Chem. Commun. *53*, 12708–12711. 10.1039/C7CC05854C.

2. Leibler, I.N.-M., Tekle-Smith, M.A., and Doyle, A.G. (2021). A general strategy for C(sp^3)–H functionalization with nucleophiles using methyl radical as a hydrogen atom abstractor. Nat. Commun. *12*, 6950. 10.1038/s41467-021-27165-z.

3. Bower, J.K., Cypcar, A.D., Henriquez, B., Stieber, S.C.E., and Zhang, S. (2020). C(sp3)-H Fluorination with a Copper(II)/(III) Redox Couple. J. Am. Chem. Soc. *142*, 8514–8521. 10.1021/jacs.0c02583.

4. Neese, F. (2018). Software update: the ORCA program system, version 4.0. Wiley Interdiscip. Rev. Comput. Mol. Sci. *8*, e1327.

5. Mandal, M., Elwell, C.E., Bouchey, C.J., Zerk, T.J., Tolman, W.B., and Cramer, C.J. (2019). Mechanisms for Hydrogen-Atom Abstraction by Mononuclear Copper(III) Cores: Hydrogen-Atom Transfer or Concerted Proton-Coupled Electron Transfer? J. Am. Chem. Soc. *141*, 17236–17244. 10.1021/jacs.9b08109.

6. Bím, D., Maldonado-Domínguez, M., Rulísek, L., and Srnec, M. (2018). Beyond the classical thermodynamic contributions to hydrogen atom abstraction reactivity. Proc. Natl. Acad. Sci. U. S. A. *115*, E10287–E10294. 10.1073/pnas.1806399115.